



Molecular Crystals and Liquid Crystals Science and Technology. Section A. Molecular Crystals and Liquid Crystals

Publication details, including instructions for authors and
subscription information:

<http://www.tandfonline.com/loi/gmcl19>

The Effect of Short-Range Orientational Order on the Nematic-Isotropic Phase Transition

S. Singh^a, T. K. Lahiri^a & K. Singh^b

^a Department of Physics, Banaras Hindu University, Varanasi, 221005,
India

^b Department of Solid State Physics (Electronics), Awadh University,
Faizabad, India

Version of record first published: 24 Sep 2006.

To cite this article: S. Singh, T. K. Lahiri & K. Singh (1993): The Effect of Short-Range Orientational Order on the Nematic-Isotropic Phase Transition, *Molecular Crystals and Liquid Crystals Science and Technology. Section A. Molecular Crystals and Liquid Crystals*, 225:1, 361-371

To link to this article: <http://dx.doi.org/10.1080/10587259308036240>

PLEASE SCROLL DOWN FOR ARTICLE

Full terms and conditions of use: <http://www.tandfonline.com/page/terms-and-conditions>

This article may be used for research, teaching, and private study purposes. Any substantial or systematic reproduction, redistribution, reselling, loan, sub-licensing, systematic supply, or distribution in any form to anyone is expressly forbidden.

The publisher does not give any warranty express or implied or make any representation that the contents will be complete or accurate or up to date. The accuracy of any instructions, formulae, and drug doses should be independently verified with primary sources. The publisher shall not be liable for any loss, actions, claims, proceedings, demand, or costs or damages whatsoever or howsoever caused arising directly or indirectly in connection with or arising out of the use of this material.

The Effect of Short-Range Orientational Order on the Nematic-Isotropic Phase Transition

S. SINGH and T. K. LAHIRI

Department of Physics, Banaras Hindu University, Varanasi-221005, India

and

K. SINGH

Department of Solid State Physics (Electronics), Awadh University, Faizabad, India

(Received January 18, 1992; in final form May 30, 1992)

A statistical mechanical perturbation theory, that is derived from our earlier work, is applied to investigate the influence of short-range orientational correlation on the thermodynamic properties of nematic liquid crystals. Two-particle orientational distribution function is used in order to account for the short-range orientational order. Numerical calculations are reported for a model system interacting via a pair potential having both repulsive and attractive parts. The repulsive interaction is represented by that between hard ellipsoids of revolution and is short-range rapidly varying potential. Dispersion forces give rise to the attractive interaction. The effect of pressure on the stability, ordering and phase transition properties is analysed and found to be in accordance with experimental observations. It is found that the short-range orientational order has strong influence on the phase transition properties and the numerical results are in better agreement with experiments as compared to mean-field results.

Keywords: Nematic, isotropic transition.

1. INTRODUCTION

The nematic phase is characterized by long-range orientational order, i.e. the molecules, on average, tend to align with their long-axes parallel to each other along a preferred direction. It is convenient to describe this order in terms of a long-range orientational order parameter which is non-zero in the less symmetric (nematic) phase and vanishes in the more symmetric (high-temperature isotropic) phase. Although in the isotropic phase long-range orientational order is absent, the molecular orientations still show correlations, which is of short-range. The existence of short-range orientational order is demonstrated by a number of pre-transitional phenomena¹ observed in the isotropic phase just above the transition temperature, e.g. scattering of light and magnetically induced birefringence. These phenomena are related to the finiteness of correlation length, defined as the distance (usually a few intermolecular distances) over which the molecular orientations are still correlated. In a molecular statistical approach using mean-field (MF) approximation the short-range correlations are neglected. The purpose of this paper is to investigate to what extent the inclusion of short-range order changes the properties of nematic-isotropic (NI) transition as compared to mean-field results.

In previous publications^{2,3} we have developed a statistical mechanical pertur-

bation theory using MF approximation to describe the equilibrium properties of nematic liquid crystals. Basic to this theory is the recognition that the predominant factor in determining the mesophase stability is geometric. Thermodynamic properties were calculated for a model system composed of molecules interacting via a pair potential having both repulsive and attractive parts. The repulsive interaction was between hard ellipsoids of revolution. The attractive potential, a function of only the centre of mass distance and the relative orientation between two molecules, was approximated by the interaction arising from the dispersion²- and quadrupole⁴-interactions between two asymmetric molecules. The relative influence of length to width ratio (x) of molecular hard core and the anisotropy in their correlation function on the nematic-isotropic transition properties were investigated. It was found that the effect of spatial and orientational pair correlations on the thermodynamic properties are quite large and the properties are extremely sensitive to the values of molecular parameters. However, the discontinuities in the order parameter, density and entropy at the nematic-isotropic transition were found to be too large. Probably one of the main short comings of the theory^{2,3} is the use of molecular field-approximation in treating the orientational coordinates. The MF treatment assumes a one-particle orientational distribution function for the molecular orientations and neglects the short-range orientational correlations. This suggests that the inclusion of short-range correlations in the theory might improve the quantitative agreement of theoretical results with experimental data.

The effect of short-range orientational order on the nematic-isotropic transition was investigated by several authors⁵⁻⁷ for a model system having only attractive part of the potential. A similar study was performed by Ypma and Vertogen⁸ using a two-site cluster (TSC) variation method^{9,10} by incorporating both intermolecular repulsions and attractions in their model.

In this paper, TSC approximation has been applied to the orientational molecular coordinates to include the short-range orientational correlations in our earlier theory² (referred to as I). The same type of investigation as that of I has been extended to analyse the influence of short-range orientational order on the thermodynamic and orientational behaviour of nematogens close to nematic-isotropic phase transition. In the following section, a brief outline of theory and the working equations are summarized. The results and discussions are given in Sec. 3.

2. THEORY AND WORKING EQUATIONS

We consider a system composed of N nematogenic molecules of axial symmetry contained in a volume V at temperature T interacting through a potential function given by

$$U_N(\mathbf{X}_1, \mathbf{X}_2, \dots, \mathbf{X}_N) = \sum_{1 \leq i < j \leq N} [U_0(\mathbf{X}_i, \mathbf{X}_j) + U_p(\mathbf{X}_i, \mathbf{X}_j)] \quad (1)$$

where the vector $\mathbf{X}_i [= (\mathbf{r}_i, \Omega_i)]$ represents both the location \mathbf{r}_i of the centre of mass of the i th molecule and its relative orientation Ω_i described by Euler's angles θ_i , ϕ_i and ψ_i . $U_0(\mathbf{X}_i, \mathbf{X}_j)$ represents the reference potential which is described by the

repulsion between the hard ellipsoids of revolution, and satisfies the relation

$$U_0(\mathbf{X}_1, \mathbf{X}_2) \equiv U_{hr}(\mathbf{r}_{12}, \Omega_1, \Omega_2) = \begin{cases} \infty, & \text{for } r_{12} \leq D(\hat{\mathbf{r}}_{12}, \Omega_{12}) \\ 0, & \text{for } r_{12} > D(\hat{\mathbf{r}}_{12}, \Omega_{12}) \end{cases} \quad (2)$$

The perturbation potential $U_p(\mathbf{X}_1, \mathbf{X}_2)$ contains the more smoothly varying long-range attractive part. We adopt following form for the attractive interaction,

$$U_p(\mathbf{X}_1, \mathbf{X}_2) \equiv U_a(\mathbf{r}_{12}, \Omega_1, \Omega_2) = \begin{cases} -r_{12}^{-6} (c_i + c_a P_2(\hat{\mathbf{e}}_1 \cdot \hat{\mathbf{e}}_2)), & \text{for } r_{12} > D(\hat{\mathbf{r}}_{12}, \Omega_{12}) \\ 0, & \text{for } r_{12} \leq D(\hat{\mathbf{r}}_{12}, \Omega_{12}) \end{cases} \quad (3)$$

$D(\hat{\mathbf{r}}_{12}, \Omega_{12})$ is the distance of closest approach of two molecules with relative orientation Ω_{12} . $\hat{\mathbf{r}}_{12}$ is a unit vector along the intermolecular axis. c_i and c_a are constants related to the isotropic and anisotropic dispersion interactions and $\hat{\mathbf{e}}_1$ and $\hat{\mathbf{e}}_2$ are unit vectors along the symmetry axes of two interacting molecules. We take following the form¹¹ for $D(\hat{\mathbf{r}}_{12}, \Omega_{12})$,

$$D(\hat{\mathbf{r}}_{12}, \Omega_{12}) = d_0 \left[1 - \chi \frac{(\hat{\mathbf{r}}_{12} \cdot \hat{\mathbf{e}}_1)^2 + (\hat{\mathbf{r}}_{12} \cdot \hat{\mathbf{e}}_2)^2 - 2\chi(\hat{\mathbf{r}}_{12} \cdot \hat{\mathbf{e}}_1)(\hat{\mathbf{r}}_{12} \cdot \hat{\mathbf{e}}_2)(\hat{\mathbf{e}}_1 \cdot \hat{\mathbf{e}}_2)}{1 - \chi^2(\hat{\mathbf{e}}_1 \cdot \hat{\mathbf{e}}_2)^2} \right]^{-1/2} \quad (4)$$

$d_0 = 2b$. Following the statistical mechanical machinery as outlined in *I*, we write the perturbation series for the Helmholtz free-energy as

$$\frac{\beta A}{N} = \frac{\beta A^{(0)}}{N} + \sum_{t=1}^{\infty} \frac{\beta A^{(t)}}{N} \quad (5)$$

where $A^{(0)}$ is the contribution of reference system and $A^{(t)}$ represents the perturbation term described by the attractive potential, t denotes the order of perturbation.

In *I* the orientational coordinates were treated in the MF approximation and it was derived that the Helmholtz free-energy (up to the first-order perturbation term) of the model system (1) can be written as

$$\frac{\beta A}{N} = B_0(\eta, T) + \frac{\beta A_{\text{orient}}}{N} \quad (6)$$

where $\beta = 1/kT$ and B_0 is the orientation independent contribution,

$$B_0(\eta, T) = \ln \rho - 1 + \frac{\eta(4 - 3\eta)}{(1 - \eta)^2} F_0(\chi) - \beta \phi_0 \quad (7)$$

and A_{orient} refers to the orientational free energy,

$$\frac{\beta A_{\text{orient}}}{N} = \langle \ln[4\pi f(\Omega)] \rangle - B_2(\eta, T) \bar{P}_2^2 \quad (8)$$

$f(\Omega)$ is the one-particle orientational distribution function, \bar{P}_2 the second Legendre polynomial long-range order parameter and $\eta (= \rho v_0, v_0$ is molecular volume) the packing fraction. The angular bracket $\langle \dots \rangle$ denotes the ensemble average over the

N-1 particles of the system. The term B_2 is defined as

$$B_2(\eta, T) = \frac{\eta(4 - 3\eta)}{(1 - \eta)^2} F_2(\chi) + \beta\phi_2 \quad (9)$$

The one-particle orientational distribution function was determined self-consistently by minimizing the free-energy,

$$f(\Omega) = \frac{\exp[2B_2\bar{P}_2P_2(\cos\theta)]}{\int d\Omega \exp[2B_2\bar{P}_2P_2(\cos\theta)]} \quad (10)$$

In the above equations,

$$\bar{P}_2 = \int f(\Omega) d\Omega P_2(\cos\theta) \quad (10a)$$

$$F_0(\chi) = (1 - \chi^2)^{-1/2} \left[1 - \frac{1}{6}\chi^2 - \frac{1}{40}\chi^4 - \frac{1}{112}\chi^6 - \dots \right] \quad (10b)$$

$$F_2(\chi) = \frac{1}{3}\chi^2(1 - \chi^2)^{-1/2} \left[1 + \frac{3}{14}\chi^2 + \frac{5}{56}\chi^4 + \frac{25}{528}\chi^6 + \dots \right] \quad (10c)$$

$$\phi_0 = \frac{1}{12} \pi x c_i^* \eta I_6(\eta) \left[A_0 + \frac{1}{5} (c_a^*/c_i^*) A_2 \right] \quad (10d)$$

$$\phi_2 = \frac{1}{12} \pi x c_i^* \eta I_6(\eta) \left[A_2 + \left(A_0 + \frac{2}{7} A_2 + \frac{2}{7} A_4 \right) (c_a^*/c_i^*) \right] \quad (10e)$$

$$I_6(\eta) = 0.333334 + 0.429911\eta + 0.241818\eta^2 \\ + 0.017573\eta^3 + 0.090841\eta^4 - 0.0171067\eta^5 \quad (10f)$$

$$\chi = (x^2 - 1)/(x^2 + 1) \quad (10g)$$

$$c_i^* = c_i/v_0^2, c_a^* = c_a/v_0^2 \quad (10h)$$

A_0 , A_2 and A_4 are constants which are tabulated in I as a function of x .

In the MF approximation used in I the molecular orientation is expressed in terms of the one-particle orientational distribution function and the short-range orientational correlation is neglected. In order to account for nearest-neighbour correlations between molecular orientations, at least a two-particle orientational distribution function is required. The TSC approximation provides a two-particle orientational distribution function of the form,

$$f(\Omega_1, \Omega_2) = (1/z_{12}) \exp \left(\frac{B_2(\eta, T)}{\gamma} P_2(\hat{e}_1 \cdot \hat{e}_2) + \frac{\gamma - 1}{\gamma} B_2(\eta, T) \right. \\ \left. \cdot \bar{S}[P_2(\hat{r}_{12} \cdot \hat{e}_1) + P_2(\hat{r}_{12} \cdot \hat{e}_2)] \right) \quad (11)$$

where γ denotes the number of nearest neighbors of a molecule.

The orientational free-energy of the model system (1) in the TSC approximation is obtained as,

$$\frac{\beta A_{\text{orient}}}{N} = -\frac{1}{2} \gamma \ln z_{12} + (\gamma - 1) \ln z_1 \quad (12)$$

where

$$z_1 = \int d\Omega \exp[2B_2(\eta, T) \bar{S} P_2(\hat{r}_{12} \cdot \hat{e})] \quad (13)$$

In the above expressions \bar{S} is a variational parameter to be determined self-consistently by minimizing the free-energy. The result is

$$\frac{1}{2} \langle [P_2(\hat{r}_{12} \cdot \hat{e}_1) + P_2(\hat{r}_{12} \cdot \hat{e}_2)] \rangle_{z_{12}} = \langle P_2(\hat{r}_{12} \cdot \hat{e}) \rangle_{z_1} \quad (14)$$

Here the thermal averages $\langle \dots \rangle_{z_{12}}$ and $\langle \dots \rangle_{z_1}$ must be evaluated, respectively, with two- and one-particle distribution functions.

The total Helmholtz free-energy per particle in the TSC approximation is given by

$$\frac{\beta A}{N} = B_o(\eta, T) - \frac{1}{2} \gamma \ln z_{12} + (\gamma - 1) \ln z_1 \quad (15)$$

All the other thermodynamic quantities such as pressure, chemical potential and entropy can readily be derived from Equation (15). In these expressions there appears a term $\langle P_2(\hat{e}_1 \cdot \hat{e}_2) \rangle_{z_{12}}$ which measures the nearest neighbors correlation between molecular orientations. This quantity is defined as short-range orientational order parameter,

$$\bar{\sigma} = \langle P_2(\hat{e}_1 \cdot \hat{e}_2) \rangle_{z_{12}} \quad (16)$$

The main difference between the TSC and MF approximations turns in the value of $\bar{\sigma}$ in the isotropic phase in which the long-range orientational order parameter vanishes but $\bar{\sigma}$ still remains finite. The short-range orientational order which is largest for a small number of nearest neighbors enables one to calculate the pre-transitional effects in the isotropic phase.⁹

The nematic-isotropic (NI) transition is located by equating the pressures and chemical potentials of the two phases

$$P_{\text{nem}}(\eta, T_{\text{NI}}, \bar{P}_{2\text{NI}}, \bar{\sigma}_{\text{NI}}) = P_{\text{iso}}(\eta_i, T_{\text{NI}}, \sigma_i) \quad (17)$$

$$\mu_{\text{nem}}(\eta, T_{\text{NI}}, \bar{P}_{2\text{NI}}, \bar{\sigma}_{\text{NI}}) = \mu_{\text{iso}}(\eta_i, T_{\text{NI}}, \sigma_i) \quad (18)$$

Keeping the pressure fixed, we get equations involving unknowns η , η_i , T_{NI} , $\bar{P}_{2\text{NI}}$, $\bar{\sigma}_{\text{NI}}$ and $\bar{\sigma}_i$. In principle, these unknown parameters can be determined by solving simultaneously Equations (10a), (16), (17) and (18). But, in practice, these equations are too complex to be solved analytically. We solve then numerically by an iterative procedure.

3. RESULTS AND DISCUSSIONS

We have investigated the influence of short-range orientational order ($\bar{\sigma}$), interaction parameters (c_i and c_a) and the length-width ratio x on the thermodynamic

and orientational behavior of nematogens close to the nematic-isotropic phase transition. Figure 1 shows the transition temperature as a function of isotropic attraction c_i for a fixed c_a . The curves are drawn for several numbers of nearest neighbors γ . The transition temperatures, for fixed c_i and c_a , are plotted as functions of γ in Figure 2. In Table I number of transition properties, at the atmospheric pressure ($pv_0/k = 1.69$ K), are compared with the results obtained for several numbers of nearest neighbors and the MF result.² The variation of density, relative density change, long-range and short-range order parameters, at the NI transition are shown in Figure 3 as a function of γ . The parameter Γ listed in Table I measures the relative sensitivity of the long-range order parameter to the volume change (at constant temperature) and the temperature change (at constant volume) and is defined as

$$\Gamma = \frac{V}{T} \cdot \frac{(\partial \bar{P}_2 / \partial V)_T}{(\partial \bar{P}_2 / \partial T)_V} = - \left(\frac{\partial \ln T}{\partial \ln V} \right)_{\bar{P}_2} = \left(\frac{\delta \ln T}{\delta \ln \rho} \right)_{\bar{P}_2} \quad (19)$$

The pressure dependence of the transition temperature (dT/dp) is determined by Clausius-Clapeyron's law.

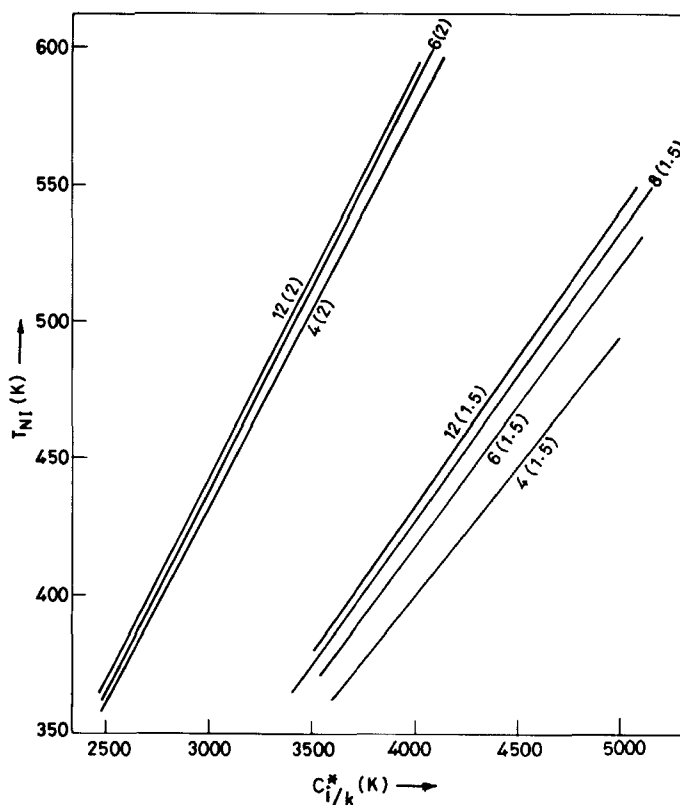


FIGURE 1 The variation of nematic-isotropic transition temperature T_{NI} , at fixed $c_i/c_a = 10$, as a function of c_i^*/k for several numbers of nearest neighbors γ . The number on the curves indicates the value of γ and the number in small brackets indicates the value of x .

TABLE I

The NI transition parameters for $x = 2.0$ as predicted by the TSC approximation for various numbers of nearest neighbors γ , and by the MF approximation \bar{P}_{2NI} is the long-range order parameter, $\bar{\sigma}_{NI}$ the short-range order parameter, η the nematic packing fraction, $\Delta\eta/\eta$ the relative density change, $\Delta\Sigma/Nk$ the transition entropy and Γ is defined in Equation (19)

c_i^*/k	c_i/c_a	γ	T_{NI}	\bar{P}_{2NI}	$\bar{\sigma}_{NI}$	η	$\Delta\eta/\eta$	$\Delta\Sigma/Nk$	$\frac{dT_{NI}}{(dp)_{NI}}$ p=1 bar	$\Gamma(T_{NI})$
2500 K	10	4	361.3	0.412	0.494	0.484	0.061	0.652	344.5	2.30
		6	367.8	0.443	0.409	0.464	0.094	0.905	412.9	2.24
		8	368.9	0.455	0.373	0.457	0.110	1.017	443.3	2.22
		12	369.7	0.467	0.339	0.451	0.126	1.127	473.6	2.19
		MF	700.5	0.747	-	0.476	0.308	3.964	393.2	2.26
		(Ref. 2)								
3000 K	20	4	400.0	0.417	0.492	0.502	0.045	0.563	280.4	2.46
		6	409.7	0.450	0.407	0.483	0.067	0.757	332.0	2.40
		8	412.5	0.463	0.371	0.476	0.078	0.841	354.4	2.37
		12	415.0	0.477	0.337	0.469	0.089	0.923	376.8	2.35
		MF	768.0	0.684	-	0.481	0.163	2.604	259.6	2.41
		(Ref. 2)								

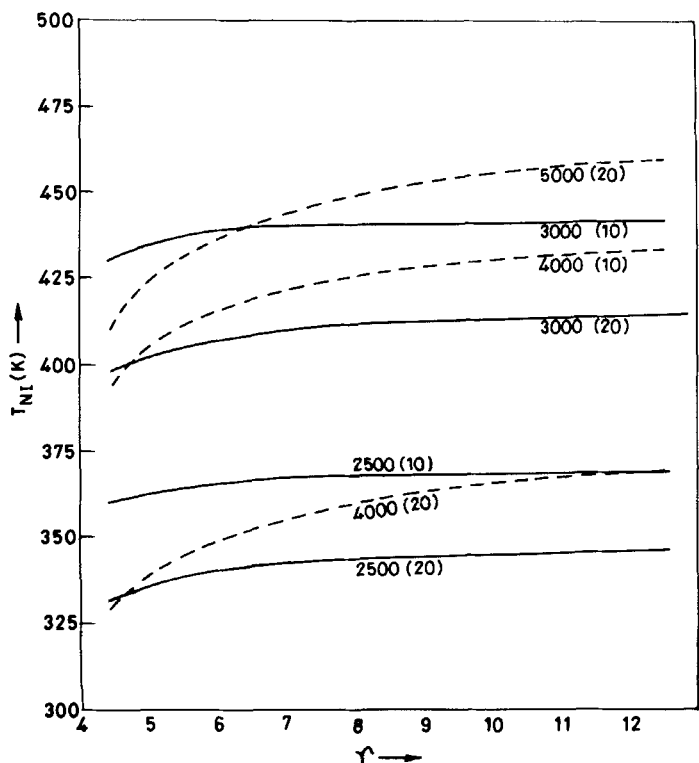


FIGURE 2 The variation of transition temperature T_{NI} , fixed c_i^*/k and c_i/c_a , as a function of numbers of nearest neighbors γ . The number on the curves indicates the value of c_i^*/k and the number in small brackets indicates the value of c_i/c_a . The dashed and solid line curves are, respectively, for $x = 1.5$ and 2.

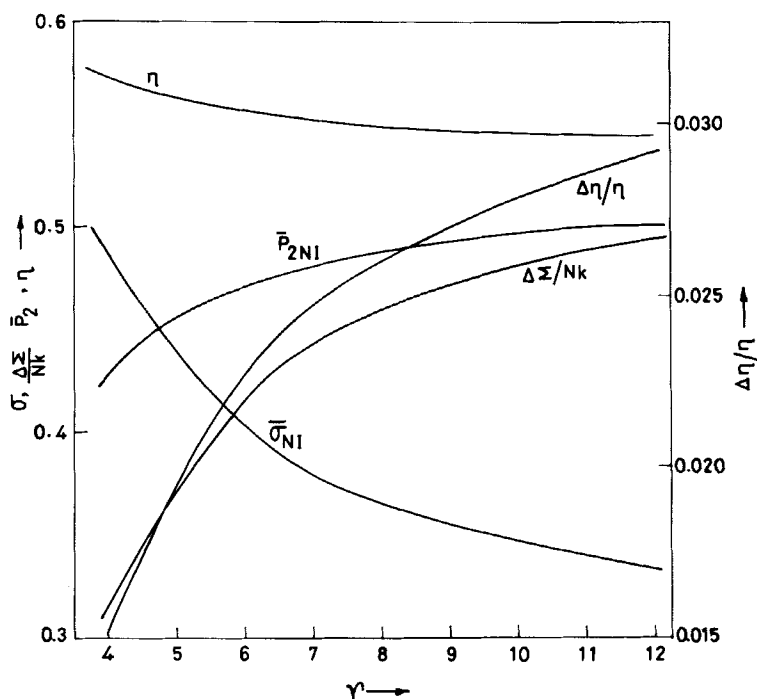


FIGURE 3 The variation of packing fraction η , long-range order parameter \bar{P}_{2NI} , short-range order parameter $\bar{\sigma}_{NI}$, and relative density change $\Delta\eta/\eta$ at the nematic-isotropic transition as a function of numbers of nearest neighbors γ for the parameters $x = 1.5$, $c_k^*/k = 4000$ K and $c_i/c_a = 10$.

From the Figures 1–3 and Table I we observe that the short-range orientational order reduces the transition temperature appreciably in comparison with the MF results. The discontinuities in the long-range order parameter, the density and the entropy at the transition decrease by the inclusion of short-range orientational correlation in the calculation. The transition is strongly influenced by the number of nearest neighbors γ . As γ increases the phase transition shifts to higher temperature, lower density with increasing discontinuities in long-range order parameter, density and entropy. The value of short-range order parameter decreases with γ but the parameter Γ remains almost unaffected.

We have studied the variation of transition properties with the strengths of potential parameters c_i and c_a for the several values of x . As physically expected we find that for a given γ with increasing x the phase transition is shifted to higher temperature, lower density, higher entropy and density changes and jump of the order parameters. Further, the calculation shows that the interaction parameters have strong influence on the transition properties. We find that the relative density change decreases as the ratio c_i/c_a increases (i.e. c_a decreases) for a given value of c_i . Though the packing fraction η increases with c_i/c_a the increase is very slow. For $c_i/c_a > 20$, it is observed that the transition properties are not very sensitive to the ratio c_i/c_a . For a given ratio c_i/c_a as c_i increases the transition temperature increases whereas the order parameters and the discontinuities in the density and entropy decrease.

Figure 4 shows the temperature dependence of the order parameters \bar{P}_2 and $\bar{\sigma}$

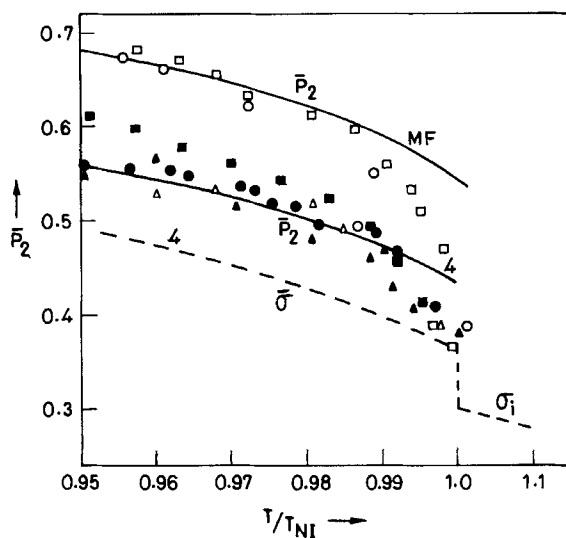


FIGURE 4 The temperature variation of order parameters \bar{P}_2 and $\bar{\sigma}$ at constant pressure ($p = 1$ bar) as obtained here (TSC approximation, $\gamma = 4$) and in I (MF approximation). The experimental points are the observed values of Rowell *et al.*¹² (● PAA, ○ PAP), Pines and Chang¹³ (■ PAA, □ PAP) and de Jeu and Claassen¹⁴ (▲ PAA, △ PAP).

at constant pressure ($p = 1$ bar). The experimental values¹²⁻¹⁴ of \bar{P}_2 for the first two members of the homologous series of di-alkoxyazoxy benzenes (PAA and PAP) are also given. The theoretical TSC curve corresponds to $x = 1.5$, $\gamma = 4$, $c_i^*/k = 4135.5$ and $c_i/c_a = 10$. The MF result ($x = 1.5$, $c_i^*/k = 3472.47$ and $c_i/c_a = 8$) is also plotted. For these curves c_i^*/k is chosen so as to reproduce the transition temperature $T \approx 409$ K. It can be seen that the agreement between the TSC result and the experimental data for PAA is quite satisfactory as compared to the MF results. The main difference between TSC and MF results is clearly seen in the isotropic phase where \bar{P}_2 vanishes but $\bar{\sigma}$ is still non-zero.

Next, we have carried out model calculations based on the experimental data for *p*-azoxyanisole (PAA). The criterion adopted in this calculation is to select the potential parameters so as to reproduce quantitatively $T_{NI} \approx 409$ K which is the experimental value for PAA. For $x = 2.0$ the results are given in Table II together with the experimental¹⁶ values. It may be seen from the Table II that as the number of nearest neighbors increases the values of packing fraction, short-range order parameter and the parameter Γ decrease whereas density and entropy discontinuities, long-range order parameter and (dT_{NI}/dp) are increased. The TSC results are closer to the experimental data as compared to the MF results. The calculated values corresponding to $\gamma = 4$ are relatively in better agreement with the experimental values. It can further be seen that the agreement between theory and experiment is getting worse with increasing number of nearest neighbors.

We have studied the pressure dependence of the thermodynamic parameters for the NI transition. The transition parameters are determined from Equations (17) and (18) at various constant values of pressure ranging from 1 bar to 600 bar. The detailed results are not given here. Figure 5 shows the transition temperature with pressure for the various numbers of nearest neighbors. Experimental values¹⁵ for

TABLE II
A comparison of NI transition parameters in *p*-azoxyanisole (PAA) and in the TSC and MF approximations. The potential parameters are chosen so as to reproduce the transition temperature $T_{NI} \approx 409$ K

Quantity	TSC Approximation				MF Approximation	Exptl. ¹⁶ PAA
	$\gamma = 4$	6	8	12		
x	2.0	2.0	2.0	2.0	2.0	~ 2.7
c_i^*/k	2830 (K)	2784	2772	2768	2663	
c_i/c_a	283 (K)	278	277	276	266	
T_{NI}	409 (K)	409	409	409	409	409
η	0.484	0.465	0.457	0.451	0.476	0.62
$\Delta\eta/\eta$	0.061	0.093	0.110	0.125	0.306	0.0035
\overline{P}_{2NI}	0.411	0.442	0.455	0.466	0.746	~ 0.40
$\overline{\sigma}_{NI}$	0.495	0.410	0.373	0.339	-	
$\Delta\Sigma/Nk$	0.651	0.901	1.017	1.124	3.946	0.218
$(\frac{dT_{NI}}{dp})_{p=1 \text{ bar}}$	344.3	411.4	443.0	472.5	391.3	43.0
$\Gamma(T_{NI})$	2.30	2.24	2.22	2.19	2.26	~ 4.0

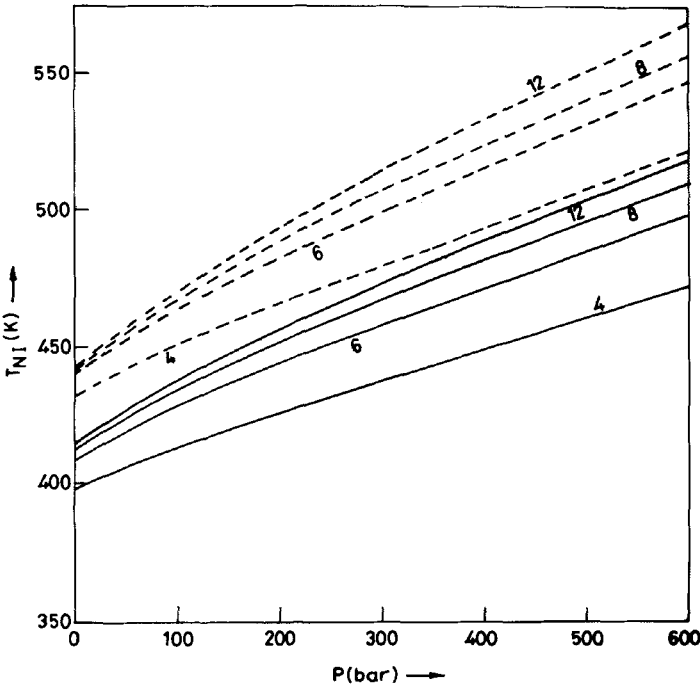


FIGURE 5 The variation of transition temperature with pressure for several numbers of nearest neighbors γ . $x = 2.0$ and $c_i^*/k = 3000$ K. The dashed and solid line curves are, respectively for $c_i/c_a = 10$ and 20 .

PAA are also given. Several general trends are evident about the variation of NI transition properties with pressure:

(i) The range of nematic phase is considerably large at constant density as compared to its stability range at constant pressure which is in agreement with experiments.

(ii) For a given x and interaction parameters as pressure increases the phase transition shifts to higher temperature and both the fractional volume change $\Delta v^*/v^*$ and transition volume v^* decrease. A decrease in the values of transition entropy and (dT_{NI}/dp) is found whereas the parameter Γ increases slightly.

(iii) At a given pressure with the decreasing values of the interaction strength ratio c_a/c_i , and fixed c_i , the values of transition temperature, transition volume, fractional volume change, transition entropy, order parameters and (dT_{NI}/dp) decrease and the parameter Γ increases.

(iv) For a given x , interaction parameters and pressure as the numbers of nearest neighbors increases the values of transition temperature, transition volume, fraction volume change, long-range order parameter, entropy change, (dT_{NI}/dp) increase whereas the short-range order parameter and Γ decrease.

In conclusion, our calculation demonstrates that the short-range orientational order has strong influence on the nematic-isotropic transition properties and that its inclusion in the molecular theory predicts the thermodynamic and orientational properties of nematic liquid crystals close to nematic-isotropic transition which are in better agreement with experiments as compared to the mean-field results.

REFERENCES

1. T. W. Stinson and J. D. Litster, *Phys. Rev. Lett.*, **25**, 503 (1970).
2. S. Singh and Y. Singh, *Mol. Cryst. Liq. Cryst.*, **87**, 211 (1982).
3. K. Singh, U. P. Singh and S. Singh, *Liq. Cryst.*, **3**, 617 (1988).
4. K. Singh and S. Singh, *Mol. Cryst. Liq. Cryst.*, **101**, 77 (1983).
5. N. V. Madhusudana and S. Chandrasekhar, *Solid State Commun.*, **13**, 377 (1973); *Pramana* **1**, 12 (1973).
6. N. V. Madhusudana, K. L. Savithramma and S. Chandrasekhar, *Pramana*, **8**, 22 (1977).
7. P. Sheng and P. J. Wojtowicz, *Phys. Rev.*, **A14**, 1883 (1976).
8. J. G. J. Ypma and G. Vertogen, *Phys. Rev.*, **A17**, 1490 (1978).
9. B. Strieb, B. H. Callen and G. Thorwiz, *Phys. Rev.*, **130**, 1798 (1963).
10. J. G. J. Ypma, G. Vertogen and H. T. Koster, *Mol. Cryst. Liq. Cryst.*, **37**, 57 (1976); *J. Phys. (Paris)*, **37**, 557 (1976).
11. B. J. Berne and P. Puchukas, *J. Chem. Phys.*, **56**, 4213 (1972).
12. J. G. Rowell, W. D. Philips, L. R. Melby and M. Panar, *J. Chem. Phys.*, **43**, 3442 (1965).
13. A. Pines and J. J. Chang, *J. Am. Chem. Soc.*, **96**, 5590 (1974).
14. W. H. de Jeu and W. A. P. Claassen, *J. Chem. Phys.*, **68**, 102 (1978).
15. R. V. Tranfield and P. J. Collings, *Phys. Rev.*, **A25**, 2744 (1982).
16. W. H. de Jeu and J. Van der Veen, *Philips Res. Rep.*, **27**, 172 (1972).